tion. To avoid the possibility of variation of detector impedance with signal level, the detector can be preceded by a ferrite isolator or an attenuator. In the latter case the sensitivity will be lower, but the author has obtained good results in varactor-diode measurements operating in this manner.

ACKNOWLEDGMENT

The author wishes to thank R. Freeman of ITT Laboratories in Madrid for his help in the composition of this short paper.

REFERENCES

[1] E. L. Ginzton, *Microwave Measurements*. New York: McGraw-Hill, 1957, p. 307.
[2] L. A. Blackwell and K. L. Kotzebue, *Semiconductor-Diode Parametric Amplifiers*. Englewood Cliffs, N. J.: Prentice-Hall, 1961, p. 138.
[3] H. M. Altschuler, "The interchange of source and detector in low-power microwave network measurements," *IEEE Trans. Microwave Theory Tech. (1964 Symposium Issue)*, vol. MTT-13, pp. 84–90, Jan. 1965.
[4] G. L. Ragan, *Microwave Transmission Circuits*. New York: McGraw-Hill, 1948, ch. 2.
[5] H. H. Skilling, *Electric Transmission Lines*. New York: McGraw-Hill, 1951, ch. 1.
[6] R. I. Sarbacher and W. A. Edson, *Hyper and Ultrahigh Frequency Engineering*. New York: Wiley, 1943, ch. 9.

Multilayer Microstrip Transmission Lines

ANDREW FARRAR, MEMBER, IEEE, AND A. T. ADAMS, SENIOR MEMBER, IEEE

***Abstract*—A method used to treat covered microstrip is extended to multilayer microstrip. Detailed results are obtained for the general three-layer problem. Series expansion and term-by-term integration are used to obtain a closed form expression for the Green's function. Matrix methods are then used to obtain the characteristic impedance. Data obtained agree closely with experiment.**

I. INTRODUCTION

Multilayer microstrip (see Fig. 1) is often used in the design of microstrip components which operate at high levels of RF power (kilowatt) or in the design of overlay microwave couplers. Hence there is a need for the basic design data for multilayer microstrip. Yamashita and Atsuki [5], [6] have treated multilayer microstrip problems by variational methods. The method of separation of variables has previously been used in the derivation of the Green's function for covered microstrip [1]. In this short paper the formulation is extended to obtain the potential distribution for multilayer microstrip in general form. The general solution for the Green's function may be completed by the inversion of an N by N matrix, where N is the number of layers, and the evaluation of an infinite integral. Once the Green's function is obtained, then the electrostatic properties of multilayer–multiconductor microstrip, such as the capacitance matrix, may be obtained by matrix methods [2], [3]. The characteristics of quasi-TEM propagation may then be approximately calculated.

Specific results are obtained for the three-layer problem. The infinite integral is evaluated by series expansion and term-by-term integration, to obtain a closed form expression for the Green's function (potential due to a line charge in three-layer microstrip). A general computer program has been written for three-layer microstrip. Results obtained by the program agree well with experiment (to within a few percent).

II. N-LAYER MICROSTRIP

Consider the microstrip shown in Fig. 1. The Green's function for this problem is derived by considering a line of charge residing on the

Manuscript received February 15, 1974; revised April 15, 1974.

A. Farrar is with the Heavy Military Electronics Systems Division, General Electric Company, Syracuse, N. Y. 13201.
A. T. Adams is with the Electrical and Computer Engineering Department, Syracuse University, Syracuse, N. Y. 13210.

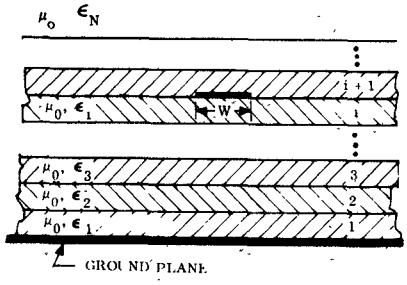

Fig. 1. Microstrip with N-layer dielectric.

ith boundary (Fig. 2). The potential V in each layer of dielectric is given by the solution of Laplace's equation

$$\nabla^2 V = 0 \tag{1}$$

which has a solution of the form

$$V = (A \sin kx + B \cos kx)(C \sin hky + D \cos hky). \tag{2}$$

Specializing the solution to the problem in Fig. 2 one can write

$$\begin{aligned}
V_1 &= \int_{-\infty}^{\infty} \cos kx (a_1 \sin hky)\, dk \\
V_2 &= \int_{-\infty}^{\infty} \cos kx (a_2 \sin hky + b_2 \cos hky)\, dk \\
&\vdots \\
V_i &= \int_{-\infty}^{\infty} \cos kx (a_i \sin hky + b_i \cos hky)\, dk \\
&\vdots \\
V_N &= \int_{-\infty}^{\infty} \cos kx a_N \exp(-ky)\, dk
\end{aligned} \tag{3}$$

where the subscript $1,2,\cdots,N$ refers to the dielectric layers $1,2,\cdots,N$. The coefficients $a_1,a_2,a_3,\cdots,a_N$ and $b_2,b_3,\cdots$, and b_{N-1} are evaluated using the following boundary conditions at the interfaces:

$$V_i = V_{i+1} \tag{4}$$

$$D_i - D_{i+1}\,|_{y=d_i} = \sigma_i = \lambda_i \delta(x)$$

where the subscript i refers to the ith layer of the dielectric where the charge is located. Substituting (3) into (4) the result in matrix form may be written as

$$\begin{bmatrix}
S_1 & -S_1 & -C_1 & \cdot & \cdot & \cdot & \cdot & 0 & 0 \\
\epsilon_1 C_1 & -\epsilon_2 C_1 & -\epsilon_2 S_1 & \cdot & \cdot & \cdot & \cdot & & \\
\cdot & \cdot & \cdot & & & & & & \\
\cdot & \cdot & \cdot & & & & & & \\
\cdot & \cdot & \cdot & & & & & & \\
0 & & & S_i & C_i & -S_i & -C_i & \cdots & 0 \\
0 & & & \epsilon_i C_i & \epsilon_i S_i & -\epsilon_{i+1} C_i & -\epsilon_{i+1} S_i & \cdots & 0 \\
\cdot & \cdot & \cdot & & & & & & \\
\cdot & \cdot & \cdot & & & & & & \\
\cdot & \cdot & \cdot & & & & & & \\
0 & 0 & 0 & \cdot & \cdot & \epsilon_{N-1} C_{N-1} & \epsilon_{N-1} S_{N-1} & e_N e^{-kd_{N-1}} &
\end{bmatrix}$$

$$\times \begin{bmatrix} a_1 \\ \cdot \\ \cdot \\ \cdot \\ a_i \\ b_i \\ b_{N-1} \\ a_N \end{bmatrix} = \begin{bmatrix} 0 \\ 0 \\ \cdot \\ \cdot \\ \cdot \\ 0 \\ \lambda \\ \hline 2\pi k \\ \cdot \\ \cdot \\ \cdot \\ 0 \end{bmatrix} \tag{5}$$

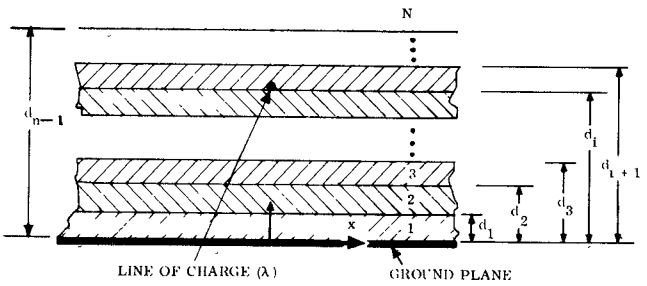

Fig. 2. Green's function geometry for N-layer microstrip.

where $S_1 = \sin hkd_1$, $C_1 = \cos hkd_1$, $\cdots$, $S_i = \sin hkd_i$, $\cdots$, $S_{N-1} = \sin hkd_{N-1}$, and $C_{N-1} = \cos hkd_{N-1}$.

Constants $a_1, a_2, \cdots, a_N$ and $b_2, b_3, \cdots, b_{N-1}$ may be obtained from (5) using matrix inversion. For single microstrip, one needs only to obtain the constants for one region, i.e.,

$$a_i = \frac{\det (G_{ai})}{\det (G)} \quad \text{and} \quad b_i = \frac{\det (G_{bi})}{\det (G)} \tag{6}$$

where the conductor lies in the ith region and $[G]$ in the square matrix in (5). Substituting (6) into the ith equation in (3) we obtain

$$V_i = \int_{-\infty}^{\infty} \cos kx \frac{[\det (G_{ai}) \sin hky + \det (G_{bi}) \cos hky]}{\det (G)} dk. \tag{7}$$

Equation (7) is the desired general Green's function for N-layer microstrip. For multiconductor problems, one must solve for the constants associated with each region in which conductors are located.

III. THREE-LAYER MICROSTRIP

Fig. 3 shows a three-layer uncovered microstrip. The line of charge is assumed to be on the boundary between region 1 and 2. Matrix equation (5) for this problem can be written as

$$\begin{bmatrix} \epsilon_1 \cos hkH & -\epsilon_2 \cos hkH & -\epsilon_2 \sin hkH & 0 \\ 0 & \epsilon_2 \cos hkE & \epsilon_2 \sin hkE & \epsilon_3 \exp(-kE) \\ \sin hkH & -\sin hkH & -\cos hkH & 0 \\ 0 & \sin hkE & \cos hkE & -\exp(-kE) \end{bmatrix} \begin{bmatrix} a_1 \\ a_2 \\ b_2 \\ a_3 \end{bmatrix} = \begin{bmatrix} \dfrac{\lambda}{2\pi k} \\ 0 \\ 0 \\ 0 \end{bmatrix}. \tag{8}$$

Only a_1 is required since the conductor is located in region 1:

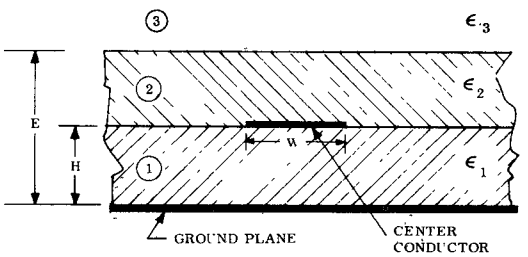

Fig. 3. Three-layer microstrip.

$$a_1(k) = \frac{Q[-\epsilon_2 \cos hk(H-E) + \epsilon_3 \sin hk(H-E)]}{-\epsilon_1\epsilon_2 \cos hkH \cos hk(H-E) + \epsilon_1\epsilon_3 \cos hkH \sin hk(H-E) + \epsilon_2^2 \sin hkH \sin hk(H-E) - \epsilon_2\epsilon_3 \sin hkH \cos hk(H-E)} \tag{9}$$

where $Q = \lambda/2\pi k$.

Substituting (7) into the first equation in (3) we obtain the Green's function for the three-layer microstrip problem in Fig. 4. Hence we have

$$V_1 = \int a_1(k) \cos kx \sin hky \, dk \tag{10}$$

where $a_1(k)$ is given by (9).

The integrand in (10) is expanded in series form to obtain, after considerable manipulation, the following expression:

$$V_1(x,y) = \frac{\lambda}{\pi(\epsilon_1 + \epsilon_2)} \left\{ -\beta \int_0^{\infty} \frac{\cos kx}{k} [\exp(-k(2E - H - y)) - \exp(-k(2E - H + y))] + \int_0^{\infty} \frac{\cos kx}{k} \cdot [\exp(-k(H-y)) - \exp(-k(H+y))] \right\} \cdot \left\{ \frac{1}{1+\alpha g} + \beta q \frac{\alpha + g}{(1+\alpha g)^2} + \beta^2 q^2 \frac{(\alpha+g)^2}{(1+\alpha g)^3} + \cdots \frac{(\beta q)^i (\alpha+g)^i}{(1+ag)^{i+1}} + \cdots \right\} \tag{11}$$

where

$$q = \exp(-2k(E-H)), \quad g = \exp(-2kH), \quad \beta = \frac{\epsilon_3 - \epsilon_2}{\epsilon_3 + \epsilon_2},$$

$$\text{and} \quad \alpha = \frac{\epsilon_1 - \epsilon_2}{\epsilon_1 + \epsilon_2}.$$

Each term of the series in (11) is expanded in a power series in g and q, the typical coefficient being A_{mn}. Then integrating term by term,

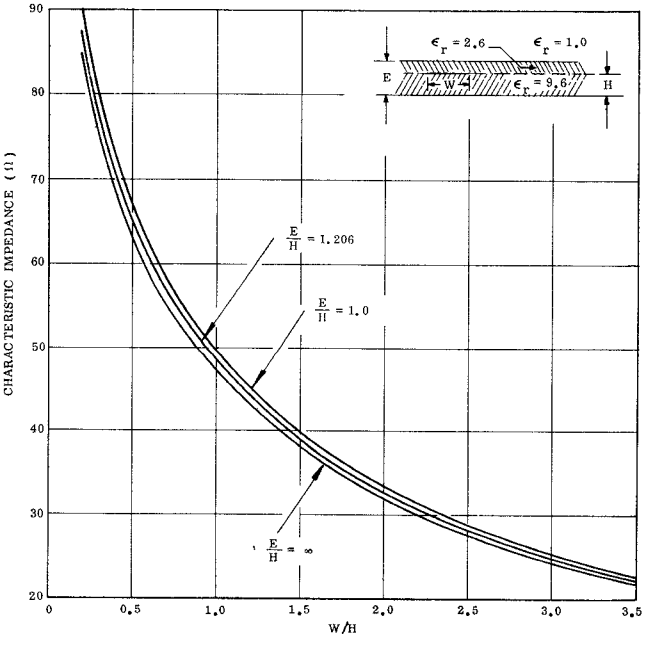

Fig. 4. Characteristic impedance for three-layer microstrip.

$$V_1(x,H) = \frac{\lambda}{2\pi(\epsilon_1+\epsilon_2)} \sum_{n=0}^{\infty} \beta^{n-1} \sum_{m=0}^{\infty} A_{mn} \cdot \left\{ -\beta \log \frac{(x/H)^2 + 4[r(n+1)+m]^2}{(x/H)^2 + 4[r(n+1)+(m-1)]^2} + \log \frac{(x/H)^2 + 4[nr+m]^2}{(x/H)^2 + 4[nr+(m-1)]^2} \right\} \quad (12)$$

where $r = ((E/H) - 1)$. The form of (12) suggests the possibility of a derivation by multiple images. The doubly infinite series in (12) converges rapidly; less than 100 terms are required. For $\epsilon_2 = \epsilon_3$ and $E = H$, (10) reduces to the Green's function for two-layer microstrip [4].

Fig. 4 shows some typical results for a three-layer problem ($\epsilon_1 = 9.6\epsilon_0$, $\epsilon_2 = 2.6\epsilon_0$, $\epsilon_3 = \epsilon_0$). The middle curve ($E/H = 1.206$) represents a three-layer microstrip currently in use. The upper and lower curves correspond to two-region problems and agree precisely with data computed from two-region programs. The middle curve agrees within better than two percent with limited experimental data available. Computation time for a typical curve is about 1 min on the GE-635 computer. Notice that as the thickness of the second dielectric layer increases, the characteristic impedance decreases.

IV. CONCLUSIONS

The multilayer multiconductor microstrip has been treated in general. The three-region microstrip has been analyzed in detail and a general computer program has been prepared. Results appear to be accurate to within a few percent.

REFERENCES

[1] A. Farrar and A. T. Adams, "A potential theory method for covered microstrip," *IEEE Trans. Microwave Theory Tech.* (Short Papers), vol. MTT-21, pp. 494–496, July 1973.
[2] R. F. Harrington, *Field Computation by Moment Methods.* New York: Macmillan, 1968.
[3] A. T. Adams, *Electromagnetics for Engineers.* New York: Ronald, pp. 166–215.
[4] P. Silvester, "TEM wave properties of microstrip transmission lines," *Proc. Inst. Elec. Eng.*, vol. 115, Jan. 1968.
[5] E. Yamashita, "Variational method for the analysis of microstrip-like transmission lines," *IEEE Trans. Microwave Theory Tech.*, vol. MTT-16, pp. 529–535, Aug. 1968.
[6] E. Yamashita and K. Atsuki, "Strip line with rectangular outer conductor and three dielectric layers," *IEEE Trans. Microwave Theory Tech.*, vol. MTT-18, pp. 238–244, May 1970.

A Low-Loss Branching Filter for Broad Widely Spaced Bandwidths

E. A. OHM, MEMBER, IEEE

***Abstract*—A waveguide filter which separates the 4-GHz band from the combined 4-, 6-, and 11-GHz common-carrier bands with a loss of only 0.05 dB is described. The input is limited to a single polarization, but dual polarizations can be accommodated by using two such filters in combination with a polarization coupler. The filter also has low insertion losses at 6 and 11 GHz: 0.1 dB and 0.06 dB, respectively, a good return loss, 32 dB, and a short length, 2½ ft. Additionally, it has high power-handling capability, good isolation properties, and good mode purity.**

INTRODUCTION

Branching networks are widely used in radio systems to connect dual-polarized common-carrier bands to a single antenna [1], but usually these networks are too long and their insertion losses are too large for satellite earth-station use. This has encouraged the development of a new network in which the key parts are a polarization coupler and a branching filter. The mode purity and feasibility of the filter in a dual-polarized feed system have been measured at 4 and 6 GHz, but these characteristics have not been completely evaluated at 11 GHz because only the 4- and 6-GHz bands were of interest in the latest series of measurements. However, the available data indicate that the filter's mode purity is sufficiently good for a dual-polarized 4-, 6-, and 11-GHz system. Such a system would also require a new type of polarization coupler, i.e., one which operates across all three bands. An appropriate coupler has been proposed [2], and deserves further investigation, but a discussion of polarization couplers is beyond the scope of this short paper. Accordingly, the couplers are mentioned only insofar as they are needed to describe the higher order mode measurements of the filter.

Manuscript received February 22, 1974; revised May 13, 1974.
The author is with Bell Laboratories, Holmdel, N. J. 07733.

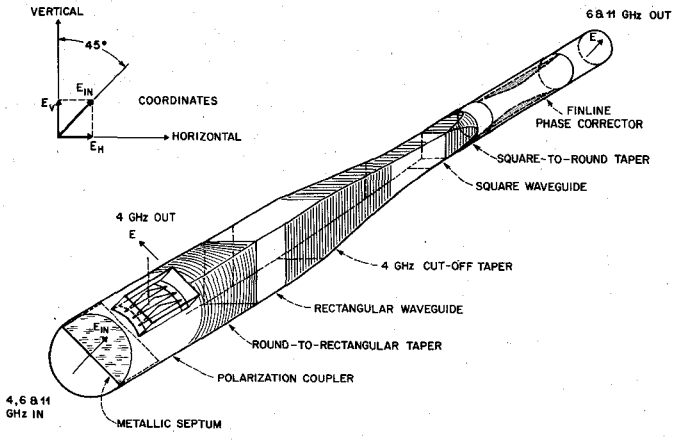

Fig. 1. Principal waveguide surfaces.

PRINCIPLE OF OPERATION

A sketch of the principal waveguide surfaces is shown in Fig. 1. At the round waveguide input on the lower left, which is dominant-mode size at 4 GHz, the dominant-mode signals are inclined 45° with respect to the vertical plane, and are transmitted straight through the polarization coupler. At the coupler output, these are resolved into equal-amplitude vertical and horizontal E-field components, which at 4 GHz are reflected by the cutoff taper, and return to the coupler with a differential phase shift of 180°. To maintain 180° across the 13.6-percent bandwidth, the phase shift is obtained partly from the differential phase shift of the rectangular waveguide, and partly from the longitudinal displacement of the vertical and horizontal walls of the cutoff taper. Adding the E-field components vectorally, the reflected dominant mode is rotated 90°. The rotated polarization is transmitted out of the filter via the side arm of the polarization coupler.

At 6 and 11 GHz (8.4- and 9.3-percent bandwidths), the equal-amplitude vertical and horizontal components are transmitted through the cutoff taper, but with substantially different phase shifts. The difference is reduced to a negligible value by further transmission through the vertically oriented finline phase corrector. As a result, the 6- and 11-GHz components at the main output, on the upper right in Fig. 1, are essentially in phase and add vectorally to yield a polarization which is parallel to that at the input.

The principle of operation is similar to that of a diplexing filter which uses two hybrids and two separate cutoff tapers [3], but here all essential operations are broader band and are performed in a single in-line waveguide.

POLARIZATION COUPLER

For the straight-through path, the coupler in Fig. 1 has a minimum return loss of 47 dB in the 4-GHz band, and 39 dB in the 6- and 11-GHz bands. Around the corner, the minimum return loss is 41 dB in the 4-GHz band. The isolation between the straight-through and around-the-corner polarizations is better than 40 dB.